

Journal of Materials Chemistry A

Accepted Manuscript



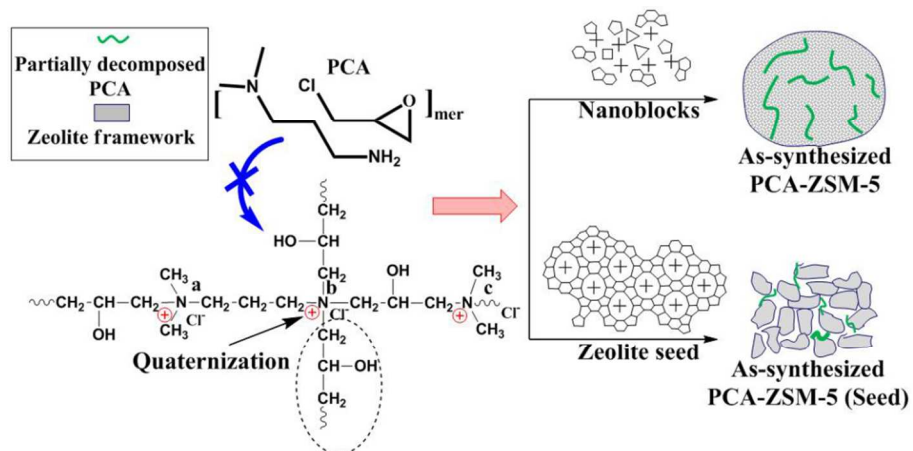
This is an *Accepted Manuscript*, which has been through the Royal Society of Chemistry peer review process and has been accepted for publication.

Accepted Manuscripts are published online shortly after acceptance, before technical editing, formatting and proof reading. Using this free service, authors can make their results available to the community, in citable form, before we publish the edited article. We will replace this *Accepted Manuscript* with the edited and formatted *Advance Article* as soon as it is available.

You can find more information about *Accepted Manuscripts* in the [Information for Authors](#).

Please note that technical editing may introduce minor changes to the text and/or graphics, which may alter content. The journal's standard [Terms & Conditions](#) and the [Ethical guidelines](#) still apply. In no event shall the Royal Society of Chemistry be held responsible for any errors or omissions in this *Accepted Manuscript* or any consequences arising from the use of any information it contains.

Graphic abstract



Partially decomposed PCA can assemble with small-sized nanoblocks to synthesize hierarchical ZSM-5, but is difficult to assemble with large-sized zeolite seeds .

Cite this: DOI: 10.1039/c0xx00000x

www.rsc.org/xxxxxx

ARTICLE TYPE

Templating Effect of an Easily Available Cationic Polymer with Widely-separated Charge Centers on the Synthesis of Hierarchical ZSM-5 Zeolite

Yicheng Zhang,^a Kake Zhu,^a Xuezhi Duan,^a Xingui Zhou^{*a} and Weikang Yuan^a⁵ Received (in XXX, XXX) Xth XXXXXXXXX 20XX, Accepted Xth XXXXXXXXX 20XX

DOI: 10.1039/b000000x

Epichlorohydrin-N,N-dimethyl-1,3-diaminopropane copolymer (PCA) has been firstly introduced as a meso-temple to successfully synthesize hierarchical ZSM-5 zeolite (PCA-ZSM-5) with mesopores of 7-50 nm in diameter by using small-sized nanoblocks. However, when its structural analogue 10 epichlorohydrin-dimethylamine polyamine (PCS) was used, the obtained ZSM-5 zeolite (PCS-ZSM-5) has lower mesoporosity than ZSM-5 nanocrystallite aggregates (NCA-ZSM-5) synthesized without meso-temple. The templating effect of the two employed cationic polymers (PCS and PCA) on the synthesis of hierarchical ZSM-5 is valuable and interesting to be evaluated, because they are easily available and have common structural characteristics that their macromolecular structure will be largely endangered by 15 the decomposition of quaternary ammonium groups in the long polymer chain. PCA entrapped in zeolite partially retains its cationic charges and macromolecular structure under hydrothermal condition and thus has a significant templating effect on the synthesis of hierarchical ZSM-5, which is benefited from the cationic centers widely separated by more than 3 carbons in PCA. However, PCS decomposes severely into small amine molecules, due to the short separation of cationic centers. Further investigation into the 20 templating effect of PCA shows that the small-sized and negatively charged nanoblocks can easily wrap and assemble with PCA and crystallize into hierarchical ZSM-5 templated by PCA. However, when using large-sized zeolite seeds to synthesize ZSM-5, PCA shows a negligible templating effect because PCA with limited charge density and low accessibility of cationic charges has insufficient interactions with zeolite seeds. The catalytic activities of PCA-ZSM-5 and NCA-ZSM-5 for acetalization of cyclohexanone 25 with methanol are inferior to that of PCS-ZSM-5 with highest number of acid sites, but the catalytic activities for aldol condensation of benzaldehyde with n-butyl alcohol follow the order of PCA-ZSM-5 > NCA-ZSM-5 > PCS-ZSM-5, consistent with the order of mesoporosity.

Introduction

Synthetic zeolites are widespread heterogeneous catalysts 30 which have gained significant popularity in oil refining and petrochemistry. However, the utilization of zeolite is usually inefficient because of the limited diffusion of reactants and products in the confined space of microporous networks and/or the accessibility of intrazeolite acid sites towards large 35 molecules.[1,2] To obtain zeolite materials with shortened diffusion path, zeolite nanocrystals,[3] exfoliated zeolites from layered precursors,[4] and surfactant-directed zeolite nanosheets[5] were synthesized through reducing the zeolite size mono- or multi-dimensionally. In comparison with 40 them, hierarchical zeolites realized by introducing additional porosity into zeolite crystal or crystal assemblies are more competitive, because they have an advantage of integrating hierarchical porosity, strong acidity and exceptional hydrothermal stability into one material. [6]

45 In the previous researches, two main strategies were extensively studied to fabricate the hierarchical zeolites. One

strategy is the demetallation treatments of premade large crystal zeolites (e.g., steaming dealumination,[7] acid dealumination[7,8] and base desilication[9]), but the etching of zeolites is often 50 accompanied by the loss of crystallinity, which leads to detrimental effects on the catalytic performance. Another strategy is dual templating method with the addition of a meso-temple besides the common zeolite structure-directing agent (SDA), which features direct creation of mesopores in zeolite during the 55 hydrothermal synthesis procedure.[10,11]

The meso-templates can be divided into hard templates and soft templates. In spite of the good versatility, hard templating route [12-15] always suffers from disadvantages such as incompatibility with zeolite synthetic gel [16] and possible 60 unconnected mesopores.[17] Accordingly, soft templates in the form of surfactants or polymers[18-20] become promising templates for the synthesis of hierarchical zeolites. Unlike the ordinary surfactant with hydrophobic long chain,[18] polymer template will not perturb the zeolite crystallization process 65 through self-assembly, because polymer does not form regular

micelles. Mesoscale polymer networks[20-28] having good compatibility with zeolite precursor during zeolite crystallization [20,26] were employed to make remarkable influences on zeolite nucleation and growth. Typically, silylated polymers have strong affinity towards zeolite domain by chemical bonding [23,24] and cationic polymers use cationic charges of high density to strongly interact with negatively charged aluminosilicate via Coulomb interaction.[25-28] In these cases, phase separation between polymer and zeolite precursor is avoided and thus mesopores in zeolites are easily templated by these polymers. Regardless of whether they are commercial or homemade polymers, regardless of whether they are derived from polymerization of suitable monomers or functionalization of reactive precursor polymers, the polymer templates are already provided prior to being added to zeolite precursor in most cases. In-situ polymerization strategy, which is carried out by mixing their respective monomers with crude materials of zeolite and conducting polymerization in the precursor solution, is also utilized to synthesize hierarchical zeolites, such as in-situ formation of crosslinked polyacrylamide hydrogels[29,30] and epoxy-resin composite.[31]

In terms of cationic polymer templating route, the strong Coulomb interactions between polymers and aluminosilicate domains are basically guaranteed due to the high density of cationic charges. In addition, the stability of cationic polymers under hydrothermal conditions of zeolite synthesis is essential to keep a mesoscale morphology and thus occupy a certain space within zeolite for mesopore generation.[26] In principle, quaternary ammonium groups, which provide cationic charges for cationic polymer,[32] can decompose via Hofmann elimination in high-temperature basic solution that is usually required in the crystallization of zeolites.[33,34] Decomposition of quaternary ammonium groups deprives the polymer of its cationic charges, but whether it also destroys the macromolecular structure depends on the position of the quaternary ammonium groups in the polymer. The previously reported cationic polymers, which are competent in templating synthesis of hierarchical zeolites,[25-28] bear the quaternary ammonium groups situated either in the polymer backbone that is also linked by other stable chemical bonds[25,26] or at the end of pendant side chains[27,28]. Even if the decomposition of quaternary ammonium groups occurs as a major reaction during hydrothermal synthesis of zeolite, the backbone chain of these polymers will not be cleaved and the resultant undesirable templating effect of these polymers on zeolite growth will be only due to weakened Coulomb interaction, rather than decreased space occupancy caused by destruction of macromolecular structure.

On the other hand, when quaternary ammonium groups serve as important linkages in the long polymer chains including backbone and very long side chain, they are the key to constructing the macromolecular structure of cationic polymer. Once the scission of C-N bonds of quaternary ammonium groups occurs, the polymer will decompose drastically and lose the cationic charges and macromolecular structure simultaneously. In other words, the considerable decomposition of quaternary ammonium groups can strongly affect both the Coulomb interaction and space occupancy, which are considered to have a synergistic effect on the cationic polymer templating synthesis of hierarchical zeolites. Numerous cationic polymers (usually

ionenes) possess the above mentioned structural characteristics[32] and respond more sensitively to the Hofmann elimination reaction than the previously reported stable cationic polymers.[25-28] Among them, two cationic polymers, epichlorohydrin-dimethylamine polyamine (PCS) and epichlorohydrin-N,N-dimethyl-1,3-diaminopropane copolymer (PCA), are easily available because they can be facilely synthesized by polymerization of common and inexpensive monomers. Besides, they are basically similar in structure so as to compare their stabilities from a structural point of view. In this regard, the two easily available cationic polymers PCS and PCA were used as meso-templates for the synthesis of hierarchical ZSM-5 zeolites for the first time. Between them, only PCA succeeds in generating mesopores within ZSM-5 zeolite, which encourages our motivation to understand the relationship between the structure and templating effect of PCA. Subsequently, the templating effect of PCA on zeolite growth was further evaluated and elucidated by exploring its sensitive response to different zeolite precursors. A comparison of catalytic performance over the obtained materials was conducted by choosing acetalization of cyclohexanone with methanol and aldol condensation of benzaldehyde with n-butyl alcohol as the probe reactions. The uncovering of the potential of PCA in this work will be important to design or select other easily available cationic polymers for the templating synthesis of hierarchical zeolites.

Experimental section

Chemicals

All reagents were used without any further purification. Tetrapropylammonium hydroxide (TPAOH, 25 wt % aqueous solution) was purchased from Shanghai Cainorise Chemicals Co., Ltd (China). N,N-dimethyl-1,3-diaminopropane (DMDAP) was from J&K Chemical. Other reagents including epichlorohydrin (ECH), N,N-dimethylamine (DMA), tetraethyl orthosilicate (TEOS) and aluminum isopropoxide (AIP) were purchased from Shanghai Lingfeng Chemical Reagent Company Ltd.

Synthesis of cationic polymers

Cationic polymer PCS or PCA was synthesized by condensation polymerization of ECH with DMA or DMDAP. The cationic polymers PCS and PCA are abbreviated as follows[35]: PC-polycation, S-secondary amine (DMA), A-asymmetrical diamine (DMDAP). The synthesis procedures of cationic polymers are followed:

1. Epichlorohydrin-dimethylamine polyamine (PCS): The linear polyamine PCS synthesized from polycondensation reaction of ECH with DMA was according to a method presented in detail elsewhere.[36,37]
2. Epichlorohydrin-N,N-dimethyl-1,3-diaminopropane copolymer (PCA): The synthesis method of PCA was adapted from a method described in a European patent.[38] To a solution of 12 g DMDAP in 16.41 g water, 9.59 g ECH was dropwise added with cooling within 60 minutes. The mixture was held at 90 °C for 60 minutes. Additional 1 g ECH was added and further stirred for 4 hours.

The obtained polymer (PCS or PCA) was recovered by precipitation with acetone and was then dried in vacuum over P₂O₅ at room temperature. The low-molecular-weight PCA

(LPCA) was also synthesized for comparison and the procedure is described in the ESI.

Because the primary amine group on DMDAP has a trifunctionality, its unselective N-alkylation with ECH may occur. The PCA is probably to have a branched structure which is very complicated and will be discussed below.

Synthesis of hierarchical zeolites

In a typical synthesis, 0.13 g AIP and 6.51 g TEOS were mixed together and stirred at room temperature for 1 h, followed by the addition of 4.19 g deionized water. After 1 minute stirring, a solution of 0.65 g PCS or PCA in 9.49 g TPAOH was added dropwise into the above mixture, followed by vigorously stirring at 30 °C for 12 hours. The addition amount of cationic polymer was determined by weight ratio of polymer to TEOS. The crystallization of the zeolite phase was carried out in a Teflon-lined autoclave at 150 °C for 48 hours under static conditions. The products were washed, air-dried and calcined at 550 °C for 6 hours to remove the SDA and polymer. The obtained materials are designated as PCS-ZSM-5 (with the weight ratio of PCS/TEOS at 0.1) and PCA-ZSM-5 (with the weight ratio of PCA/TEOS at 0.1). For comparison, ZSM-5 sample was also synthesized without adding polymer under the similar procedures, which is similar in recipe to the previously reported ZSM-5 nanocrystallite aggregates [23] and is accordingly designated as NCA-ZSM-5. ZSM-5 sample was synthesized with LPCA under the similar procedures, which is designated as LPCA-ZSM-5 (with the weight ratio of LPCA / TEOS at 0.1). PCA-Silicalite-1 was also synthesized under the similar procedures to PCA-ZSM-5 except for no use of aluminium resource.

Characterizations

Molecular weight distributions of the polymers were measured by Waters 1525 GPC with water as mobile phase using Polyethylene Oxide (PEO) samples as standardstabs. X-ray diffraction (XRD) patterns were recorded with a Rigaku D/Max2550V diffractometer, with CuK α Radiation at 40 kV and 100 mA. The XRD patterns were collected in the range of 5–50° in 2 θ / θ scanning mode with a 0.02° step and scanning speed of 12 degree/min. Nitrogen adsorption-desorption isotherms were measured on an ASAP 2010 (Micromeritics, USA) analyzer at 196 °C after the samples were degassed under vacuum for several hours at 250 °C. Specific surface area was calculated by the BET (Brunauer-Emmett-Teller) method based on the adsorption data at P/P_0 of 0.05 - 0.2. The micropore volume was calculated using t-plots at P/P_0 of 0.1 - 0.4 (de Boer). The pore size distribution was calculated from the adsorption branch using the BJH (Barrett-Joyner-Halenda) method, and total pore volume was obtained from the adsorption at $P/P_0 = 0.99$. Scanning electron microscopy (SEM) images were recorded on a Nova NanoSEM 450 at an acceleration voltage of 5 kV. Transmission electron microscopy (TEM) images and selected area electron diffraction (SAED) were obtained on a JEM-2100 instrument operated at 200 kV. All samples subjected to TEM measurements were dispersed in ethanol ultrasonically and were dropped on copper grids. Also, powders were microtomed to get ultrathin sections of particles. First, the zeolite particles were embedded directly in Spurr's epoxy resin that was polymerized at 70 °C for 16 hours. Then, ultrathin sections (thickness about 70 nm) were cut on

Leica Ultracut UCT equipped with a Drukker diamond knife, and the sections were picked up on holey carbon film on copper grids. Solid state ^{13}C MAS NMR spectra were obtained on a Bruker AVANCE III 500 NMR spectrometer operating at a spinning frequency of 125.72 MHz. The ^{13}C chemical shifts were referenced to tetramethylsilane. Solid state ^{27}Al MAS NMR spectra were recorded on the same spectrometer operating at a spinning frequency of 130.28 MHz. The ^{27}Al chemical shifts were referenced to a 1.0 M solution of aluminum nitrate. ^{13}C NMR spectra were recorded on a Bruker AVANCE III 400 spectrometer. Thermogravimetric analysis (TGA) was performed on a Perkin-Elmer Pyris 1 TGA instrument at a heating rate of 10 °C min $^{-1}$ in an air flow. The particle size distribution of the zeolite seeds was characterized by dynamic light scattering (DLS). Temperature programmed desorption of ammonia (NH $_3$ -TPD) was performed on an apparatus TP-5080 (Tianjin Xianquan Technology Development Co., Ltd.). The sample (70 mg) was heated up to 500 °C using He (30 mL min $^{-1}$) to remove adsorbed components and then cooled down to 50 °C. Pure NH $_3$ was injected until adsorption saturation was reached. Subsequently, the system was flushed with He at a flow rate of 30 mL min $^{-1}$ for 1 hour. The temperature was ramped up to 600 °C at a rate of 10 °C min $^{-1}$. A thermal conductivity detector (TCD) was used to measure the desorption profile of NH $_3$. Elemental analysis for the Si/Al ratio was performed with inductively coupled plasma optical emission spectroscopy (ICP-OES) using a SPECTRO ARCOS ICP Spectrometer.

Catalytic Reactions

In the acetalization of cyclohexanone, 0.2 g cyclohexanone and 4 g methanol were charged with 25 mg catalyst in a 25 mL round bottom flask with a reflux condenser and a magnetic stirrer. The reaction was carried out at 50 °C under continuous magnetic stirring. The products were collected by using a microsyringe and analyzed by a gas chromatograph with an SE-30 column and N $_2$ as carrier gas. The conversion was calculated based on cyclohexanone. Aldol condensation of benzaldehyde with n-butyl alcohol was carried out under N $_2$ in a three-necked flask equipped with a reflux condenser and a magnetic stirrer. In a typical run, 2.65 g of benzaldehyde, 7.4 g of n-butyl alcohol and 0.1 g of catalyst were mixed with continuous stirring, and then the reaction temperature was raised to and kept at 80 °C. The products were collected by using a micro-syringe and analyzed by a gas chromatography with an SE-30 column and N $_2$ as carrier gas. The product was further confirmed by GC-MS. The conversion was calculated based on benzaldehyde.

Results and discussion

ZSM-5 zeolites templated by PCS and PCA

The GPC profiles of cationic polymers PCS and PCA are provided in Fig. S1. PCS has a low molecular weight (Mn=1857) due to the limited polymerization degree of a linear structure,[37] but is sufficient to possess a mesoscale morphology required by generating mesopores in zeolite.[23] PCA has a high molecular weight (Mn=88622), implying the high polymerization degree of a branched polymer.

The above two cationic polymers were used to hydrothermally synthesize PCS-ZSM-5 and PCA-ZSM-5 zeolites, respectively,

which are in comparison with the NCA-ZSM-5. The three materials were characterized by XRD as shown in Fig. 1a. All three materials exhibit the characteristics of the MFI type structure any crystalline impurity phases.[39] The average crystallite sizes of the three materials calculated by the Scherrer equation are provided in Table 1. Compared with NCA-ZSM-5, both PCS-ZSM-5 and PCA-ZSM-5 have large crystal size, indicating that the addition of cationic polymer increases the crystal domains.

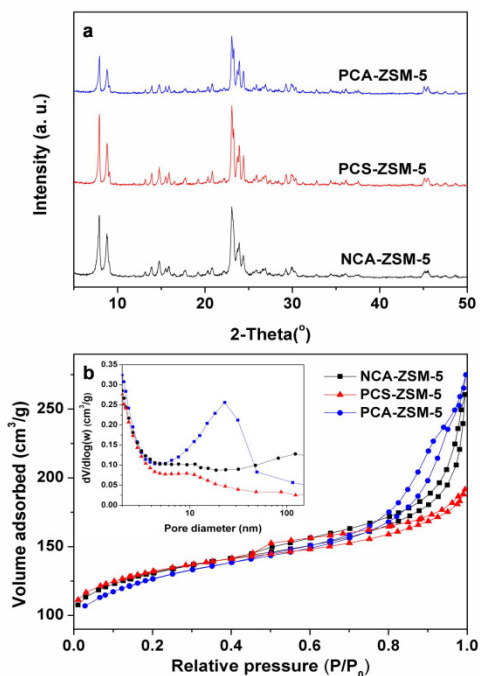


Fig. 1 (a) XRD patterns and (b) N_2 adsorption-desorption isotherms and the corresponding pore size distribution (inset in b) of NCA-ZSM-5, PCS-ZSM-5 and PCA-ZSM-5.

The mesoporosity was characterized by nitrogen adsorption-desorption measurement (Fig. 1b). The high nitrogen uptakes at relative low pressures ($P/P_0 < 0.1$) in all materials demonstrate the micropore-containing properties. Although NCA-ZSM-5 contains a certain proportion of mesopores, its BJH-derived pore size distribution (PSD) is rather broad and lacks a clear peak (Fig. 1b inset). PCS-ZSM-5 also has no PSD peak (Fig. 1b inset) and even has a smaller adsorption volume than NCA-ZSM-5, indicating that the addition of PCS has decreased the mesoporosity. Fortunately, PCA-ZSM-5 exhibits a significant increase of nitrogen adsorption and a broad hysteresis loop at relative pressures of 0.7-0.95 (Fig. 1b), due to the capillary condensation inside mesopores. This sample shows a broad distribution of mesopores ranging between 7 and 50 nm with a maximum at about 25 nm (Fig. 1b inset). The textural properties are tabulated in Table 1. Compared with NCA-ZSM-5 ($0.27 \text{ cm}^3/\text{g}$), PCA-ZSM-5 has a slight increase in mesopore volume ($0.32 \text{ cm}^3/\text{g}$), while PCS-ZSM-5 has an obvious decrease ($0.17 \text{ cm}^3/\text{g}$).

NCA-ZSM-5 synthesized without adding polymer exhibits aggregation of small crystallites (SEM, Fig. 2a and 2b), similar to the previous research.[23] As revealed in SEM (Fig. 2c and 2d) and TEM images (Fig. 3a and 3b), the bulk zeolite particles (400-

600 nm) of PCS-ZSM-5 possess regular shape, smooth surface and compact texture, showing the lack of mesopores. Compared with NCA-ZSM-5, PCS-ZSM-5 exhibits an increase in particle size and a loss of mesoporosity. Therefore, the cationic PCS is considered to exert a negligible templating effect on zeolite growth and thus is inappropriate for templating mesopores in ZSM-5. When PCA was used as the template, the resultant PCA-ZSM-5 also has increased particle size (above 500 nm), but displays a fluffy texture (Fig. 2e, 2f and 3c). The particles contain large proportion of mesopores open at the external surface (Fig. 2e and 2f). The edge of a particle (Fig. 3d), which is relatively thin to have a good contrast TEM image, is comprised of partially sintered assemblies of nanozeolites rather than amorphous particles, as indicated by the lattice fringe (Fig. 3d inset). The intra-zeolitic texture of the PCA-ZSM-5 particles is shown by the morphology of ultrathin sections ($\sim 70 \text{ nm}$). As illustrated in Fig. 3e and 3f, the big particle has broken into small fragments. The ultrathin sections are clearly not nanocrystal aggregates but contain many mesopores (bright spots) that should be imprinted by PCA. The dot pattern of selected area electron diffraction (SAED) of any ultra-thin section indicates the single crystalline nature of these sections (Fig. 3f inset). Both PCS and PCA stimulate the formation of large zeolite particles, but only cationic PCA can generate well-defined mesopores within the particles, showing an efficient templating effect on zeolite growth. Besides, compared with NCA-ZSM-5, both PCS-ZSM-5 and PCA-ZSM-5 have a higher yield of zeolite crystals, due to the larger particle size induced by polymers. The low mesoporosity of PCS-ZSM-5 and low yield of NCA-ZSM-5 serve as a foil to the advantage of PCA-ZSM-5.

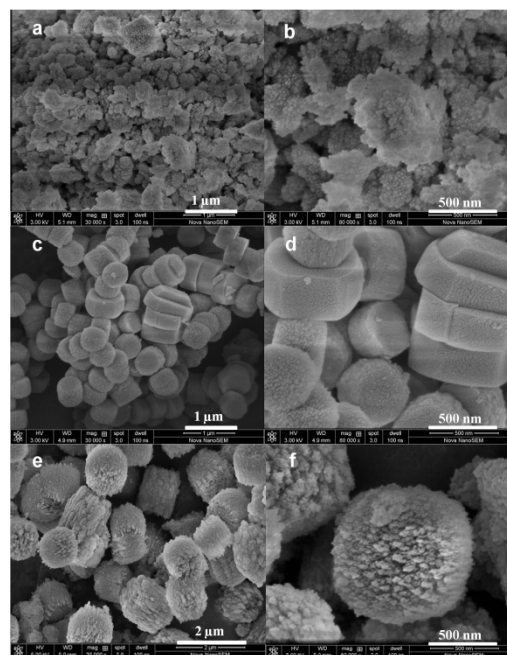


Fig. 2 SEM images of (a and b) NCA-ZSM-5, (c and d) PCS-ZSM-5 and (e and f) PCA-ZSM-5.

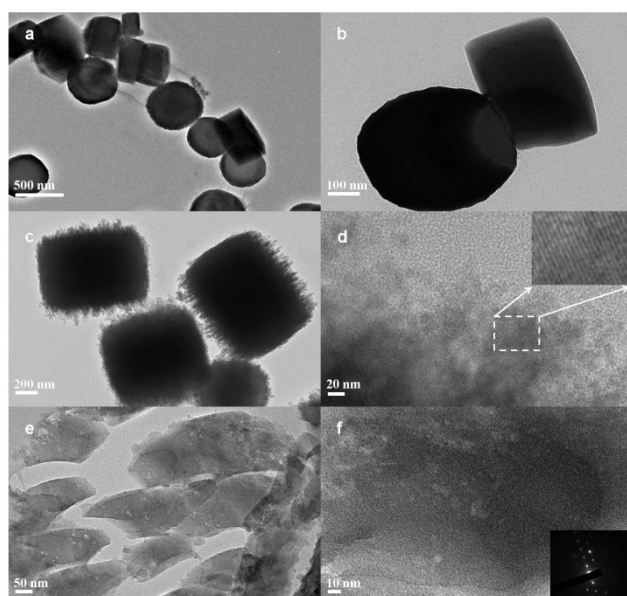


Fig. 3 TEM images of (a and b) PCS-ZSM-5, (c and d) PCA-ZSM-5 and (e and f) ultrathin sections of PCA-ZSM-5. Inset in (f) is the corresponding electron diffraction pattern.

Table 1 Textural properties obtained by nitrogen physisorption experiments^a

Sample	S_{BET} (m^2/g)	V_{total} (cm^3/g)	V_{micro} (cm^3/g)	V_{meso} (cm^3/g)	Crystal size (nm)
NCA-ZSM-5	447	0.39	0.12	0.27	53.5
PCS-ZSM-5	458	0.30	0.13	0.17	79.9
PCA-ZSM-5	437	0.43	0.11	0.32	70.1

^a S_{BET} is calculated from Brunauer–Emmett–Teller method; V_{total} is evaluated at $P/P_0=0.99$; V_{micro} is calculated from t -plot method; $V_{\text{meso}}=V_{\text{total}}-V_{\text{micro}}$; Average crystal size is determined using Scherrer's equation for the peaks at 2θ values of 7-10.

In addition, when we exchanged the high-molecular-weight PCA for low-molecular-weight PCA (LPCA, $M_n=2681$, Fig. S1), the obtained LPCA-ZSM-5 sample also shows hierarchical structure. As shown in Fig. S2 and S3, the crystalline LPCA-ZSM-5 exhibits similar isotherm shape and morphology to PCA-ZSM-5 synthesized with high-molecular-weight PCA. However, the broad distribution of mesopore diameters in the LPCA-ZSM-5 is within 6-30 nm and centered at around 13 nm (Fig. S2b, inset), corresponding to the smaller molecular weight of LPCA. Besides, the possible 3D geometry of long chain polymers may also influence the hydrodynamic radius of the branched PCA, leading to different sizes of mesopores in ZSM-5.

When PCA was used as the meso-temple to synthesize pure silica MFI structure by using TEOS as silica source, the obtained PCA-Silicalite-1 shows poor mesoporosity, as indicated by the type I (Langmuir) isotherm (Fig. S4b) and smooth zeolite surface (Fig. S5). The negligible templating effect of PCA in generating mesopores in Silicalite-1 is because that the neutral silica species can not strongly interact with positively charged PCA. Similarly, the previous research [40] reported that the alkoxysilylated cationic surfactant (TPOAC), which is widely applied in the synthesis of hierarchical zeolite, failed to synthesize hierarchical Silicalite-1 due to the weak interactions between the surfactant

with limited cationic charges and the neutral siliceous framework. Therefore, the presence of aluminium source in the zeolite precursor is largely contributable to the efficient generation of mesopores in PCA-ZSM-5, indicating the important role of Coulomb interaction.

The NCA-ZSM-5, PCS-ZSM-5 and PCA-ZSM-5 have different physical properties from each other, implying different roles of polymers in zeolite crystallization. The state of polymers within the as-synthesized samples was explored by ^{13}C MAS NMR. As shown in Fig. S6, as-synthesized PCA-ZSM-5 exhibits no well-defined peak assigned to carbon atom of intact PCA. In addition to the intensive TPA^+ peaks at 11, 16 and 63 ppm, signals between 40 and 60 ppm can be assigned to newly formed carbon species after the decomposition of PCA or original PCA structure. If there is intact PCA in the sample, its characteristic peaks can not be distinguished due to its low concentration in sample and the interference of the intensive peaks of TPA^+ and signals of decomposed products. It is almost the same case for the state of PCS in as-synthesized PCS-ZSM-5 (Fig. S7). Consequently, by using ^{13}C MAS NMR, the occurrence of decomposition of PCA and PCS is confirmed, but the decomposition degree of macromolecular structure can not be estimated. As mentioned above, the structure characteristics of PCS and PCA determine that its macromolecular structure will undergo destructive decomposition once many quaternary ammonium groups are decomposed. After the polymer largely loses the original macromolecular structure, the residual segments may exist in both zeolite and mother liquor and do not necessarily have the same state. Although the Hofmann elimination reaction is the target reaction, other reactions, which do not destroy macromolecular structure but may influence functional groups, can not be ruled out. Therefore, the cationic polymers employed in our work is very difficult to investigate as comparison with the previously reported polymers, whose macromolecular structure after decomposition of some quaternary ammonium groups are certainly retained and entirely entrapped in zeolite [25-28].

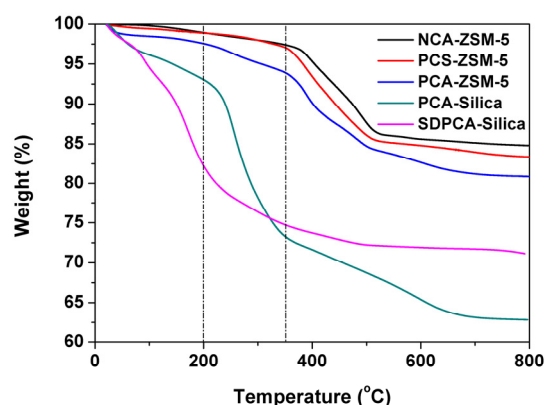


Fig. 4 Thermogravimetric analysis (TGA) curves of as-synthesized form of NCA-ZSM-5, PCS-ZSM-5 and PCA-ZSM-5, PCA-Silica (extracted from Fig. S8) and SDPCA-Silica.

The state of cationic polymer in zeolite crystal can be further verified by thermogravimetric analysis (TGA). Prior to investigating the as-synthesized zeolites, we have synthesized

PCS-Silica and PCA-Silica composites to record the thermal decomposition of the corresponding intact polymer. As shown in Fig. S8, both PCS-Silica and PCA-Silica have three comparable thermal decomposition steps. The weight loss below 180 °C can be attributed to the release of adsorbed water. The large weight losses within 200-350 °C and above 350 °C correspond to the initial and further decomposition of PCS or PCA, respectively.

Then TGA was carried out to explore the state of polymer in the three as-synthesized zeolite samples, complementing to the results obtained by ^{13}C MAS NMR. As illustrated in Fig. 4, PCS-ZSM-5 shows a weight loss of 16.7%, and PCA-ZSM-5 19.1%, which are both larger than that of NCA-ZSM-5 (15.2%). The small weight losses below 180 °C for all samples are attributed to the removal of water. The region at 400-510 °C corresponds to the decomposition of TPA^+ cations retained inside the micropores. The region above 510 °C belongs to the complete elimination of organic templates. Between 200 and 350 °C, PCA-ZSM-5 displays an increased weight loss compared with NCA-ZSM-5, which is similar to the initial decomposition of intact PCA in PCA-Silica (Fig. 4 or S8). After initial decomposition, the residual PCA segments will undergo further decomposition above 350 °C, which is similar to that of intact PCA and overlaps with that of TPA^+ cations (Fig. 4). The results indicate that the residual PCA segments entrapped within the PCA-ZSM-5, which is indirectly confirmed by ^{13}C MAS NMR, have a partially preserved macromolecular structure and thus also exhibit initial decomposition step at 200-350 °C. Therefore, the residual PCA segments (partially decomposed PCA) are still able to template mesopores in PCA-ZSM-5. In addition, low-molecular-weight PCA (LPCA) used to template smaller mesopores in LPCA-ZSM-5 also exhibits a similar case (Fig. S9).

From another standpoint, the TGA profile of severely decomposed PCA (SDPCA) should be explored so that the organics in PCA-ZSM-5 can be more clearly identified as partially decomposed PCA (PDPCA). We mixed intact PCA as the only organic compound with aluminosilicate gel and hydrothermally treated them under highly alkaline (pH=14) and high-temperature (170 °C) conditions for 24 hours. The precipitate and mother liquor were stirred and heated to get a dry solid containing all the organics (See ESI), which was analyzed by TGA as shown in Fig. 4. Compared with PCA-Silica containing intact PCA (Fig. 4), SDPCA-Silica displays the largest weight loss below 200 °C, rather than at 200-350 °C, which should be mainly assigned to the decomposition of SDPCA that has no macromolecular structure. The second largest weight loss of SDPCA-Silica at 200-350 °C is reasonably assigned to the further decomposition of SDPCA. Therefore, the harsh hydrothermal condition has made intact PCA undergo severe decomposition into small molecules. The comparison between PCA-Silica and SDPCA-Silica indicates that intact PCA begins to decompose at an obviously higher temperature region (200-350 °C) than SDPCA (below 200 °C). The high proportion of weight loss at 200-350 °C is an important feature of the presence of macromolecular structure that possessed by intact PCA or PDPCA. In retrospect, the weight loss at 200-350 °C of as-synthesized PCA-ZSM-5 occupies a higher proportion than that below 200 °C (mainly caused by removal of water), supporting the conclusion that the organics entrapped within PCA-ZSM-5 is

PDPCA. The macromolecular structure can be preserved in PDPCA because the number of decomposed quaternary ammonium groups is not very large.

Unlike PCS-Silica composite (Fig. S8), PCS-ZSM-5 has no recognizable weight loss at 200-350 °C (Fig. 4), owing to the severe decomposition of PCS during zeolite crystallization, which validates the negligible templating effect of PCS on the growth of PCS-ZSM-5. However, the additional ^{13}C signals (Fig. S7) and the larger weight loss of PCS-ZSM-5 than that of NCA-ZSM-5 confirm the presence of carbon species besides TPA^+ . It can be explained that the decomposed PCS molecules (amine molecules) are small enough to be occluded in the micropores of zeolite, resulting in their high decomposition temperature.

Structural factors controlling the templating effect of PCS and PCA during zeolite crystallization

PCS and PCA have differences at molecular level, which is conducive to the understanding of their templating effects in the zeolite synthesis. The synthesis routes of cationic polymers and the corresponding zeolites are schematically described in Fig. 5. Herein, we attempt to elucidate the relationship between the structure characteristics and templating effects of PCS and PCA during zeolite crystallization. The dark brown mother liquor of PCS-ZSM-5 is mainly due to the decomposition of PCS into small amine molecules via Hofmann elimination in high-temperature basic solution. Similar result was also reported by Ryoo's work [41] that the decomposition of $\text{C}_{22-3}\text{N}_2$ at 140 °C could be ascribed to the short $-\text{C}_3\text{H}_6-$ spacer which was insufficient to separate the charges between the two quaternary nitrogen atoms (cationic centers). In the structure of PCS shown in Fig. 5, the secondary amine group on DMA have to be quaternized by ECH to construct PCS, resulting in the formation of $-\text{CH}_2\text{CH}(\text{OH})\text{CH}_2-$ spacer between two quaternary nitrogen atoms (N,N-dimethyl-2-hydroxypropylammonium chloride as repeat unit). This short spacer is more unfavourable for the separation of charges between adjacent cationic centers than $-\text{C}_3\text{H}_6-$, because it contains an extra hydroxyl group as weak electron withdraw group on a carbon beta to the quaternary nitrogen atom. Therefore, the easy and fast decomposition of quaternary ammonium groups in the backbone will create molecules not larger than the spacer, inevitably destroying the macromolecular structure of PCS.

Although PCA has a complicated structure, which is not directly described in Fig. 5, we just need to focus on the distance between cationic centers that affects the stability of PCA during zeolite crystallization. To avoid the disadvantage of PCS, we expect PCA to have more than three carbons to separate adjacent cationic centers. Fortunately, it is permitted in principle because that a tertiary amine group and a primary amine group at both ends of DMDAP share the responsibility for connecting with ECH to construct PCA and the latter is not necessarily to be quaternized. If, on the contrary, the nitrogen atom on Position b (the primary amine group on DMDAP, Fig. 5) is unfortunately quaternized by three ECH molecules, there will be two pairs of adjacent quaternary nitrogen atoms (Position a, b and c) linked by the short spacers $-\text{CH}_2\text{CH}(\text{OH})\text{CH}_2-$ (derived from ECH) and $-\text{C}_3\text{H}_6-$ (derived from DMDAP), respectively, which will promote the undesired decomposition of quaternary ammonium groups and thus give rise to an instability similar to that of PCS.

Although the quaternization by ECH is considered to be theoretically possible,[42] it is probable to restrict the overalkylation of primary amine groups (Position b) on DMDAP. In other words, the N-alkylation of the primary amine groups can be controlled at secondary or tertiary stage to prevent quaternization. The long $-\text{CH}_2\text{CH}(\text{OH})\text{CH}_2-$ chains or even longer polymer chains (already attached to Position b) can sterically hinder the further N-alkylation, which is a more severe steric factor than that caused by short alkyl groups.[43] Therefore, the free ECH molecule is preferred to quaternize the tertiary amine group (Position a or c) on DMDAP which has only two small methyl groups, rather than the amine group connected by long chains (Position b). Moreover, the limited quantity of ECH molecules (molar ratio of ECH to DMDAP is smaller than 1: 1), which is far less than the full functional equivalency of DMDAP, may also minimize the possibility of quaternization of primary amine group (Position b) on DMDAP. Although PCA still undergoes decomposition during zeolite crystallization, its wide separation of cationic centers largely decelerates the Hofmann elimination reaction. Therefore, PCA is considered to have relatively lower decomposition rate and higher stability than PCS during zeolite crystallization. Considering the merits of creating more-than-three-carbon spacers and involving facile route and inexpensive monomers, the polymerization strategy of PCA is advantageous over many counterparts including that of PCS.[32]

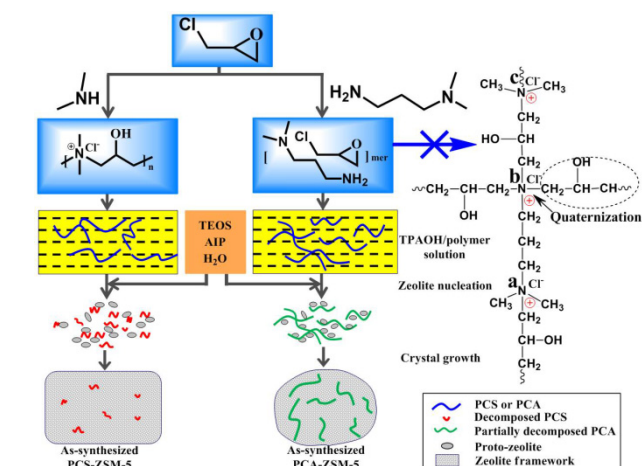


Fig. 5 Proposed synthesis route for PCS-ZSM-5 and PCA-ZSM-5.

In previous literatures, [42,44] a cationic polymer molecule synthesized with ECH and DMA as monomers and low amount of DMDAP as a crosslinker has achieved a combination of PCA and PCS segments, but the high content of PCS segment makes the polymer exhibit more properties of pure PCS. Therefore, the synthesis of PCA in our work is equivalent to complete elimination of the PCS segments in their polymer. Besides, its proposed structure shows that the N-alkylation of primary amine groups stops at the tertiary stage (di-N-alkylation),[42,44] providing straightforward evidence for a branched PCA structure (Fig. S10a). In this branched structure with 3D geometry of long chain polymers, quaternary ammonium groups situated in both backbone and long side chain serve as key linkages for PCA, and

their decomposition still largely endangers the macromolecular structure of PCA. However, in the European patent,[38] an idealized structure of PCA is proposed to be generated by mono-N-alkylation of primary amine (Fig. S10b). In this linear structure, PCA has a well-defined backbone chain carrying all the cationic charges (Fig. S10b), very similar in structure to PCS. The actual PCA is close to the branched structure, but may contain some segments of the linear structure. Both kinds of structures achieve the non-occurrence of quaternization of primary amine group on DMDAP. Moreover, the cationic charge density of PCA is undoubtedly smaller than that of PCS and is sufficient to assist the efficient interactions between PCA and aluminosilicate domains in the synthesis of PCA-ZSM-5.

Effect of zeolite precursor on synthesis of hierarchical ZSM-5 zeolites

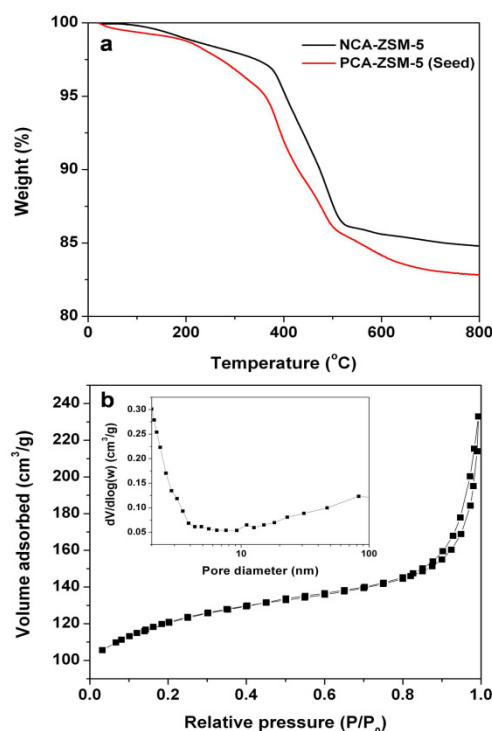
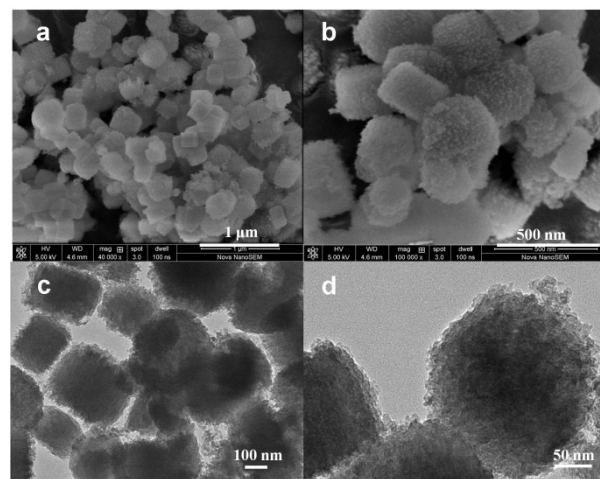


Fig. 6 (a) Thermogravimetric analysis (TG) curves of as-synthesized NCA-ZSM-5 (extracted from Fig. 4) and PCA-ZSM-5(Seed); (b) N_2 sorption isotherms and (inset in b) the corresponding pore size distribution of PCA-ZSM-5(Seed).

When the zeolite was synthesized using pre-crystallized zeolite seeds instead of TEOS, the obtained crystalline PCA-ZSM-5 (Seed) (Fig. S11) also exhibits a small weight loss at 200-350 °C (Fig. 6a), attributable to the initial decomposition of partially decomposed PCA. Similar to the case of PCA-ZSM-5, the ^{13}C MAS NMR spectrum of as-synthesized PCA-ZSM-5 (Seed) does not clearly show peaks assigned to intact PCA but confirms the presence of additional carbon species (Fig. S6). The results indicate that PCA also partially retains its macromolecular structure during the synthesis of PCA-ZSM-5 (Seed). The isotherm of PCA-ZSM-5 (Seed) exhibits an obvious uptake above

$P/P_0 = 0.8$ (Fig. 6b), and the calculated PSD (above 50 nm, Fig. 6b inset) is very distinct from that of PCA-ZSM-5 (7-50 nm). This result shows the presence of interparticle mesopores which are not templated by PCA. Specifically, the mesopores are derived from void spaces among the primary crystals zeolite within a fluffy particle (Fig. 7). The primary crystals grow from zeolite seeds and have high degree of intergrowth, resulting in their hardly observed edges (Fig. 7c and d). There are even some particles with smooth surface (Fig. 7a), suggesting that the zeolite seeds have fused into large crystal without being templated by PCA. The residual PCA segments incorporated in this sample are not capable of generating mesopores, but are considered to have a certain effect on the formation of hierarchical zeolite.



60 Fig. 7 (a and b) SEM images and (c and d) TEM images of PCA-ZSM-5 (Seed).

Compared with severely decomposed PCA in SDPCA-Silica (Fig. 4), PCA can partially keep its macromolecular structure in as-synthesized PCA-ZSM-5 and PCA-ZSM-5 (Seed), which is confirmed by TGA results rather than ^{13}C MAS NMR. The non-severe decomposition of PCA is resulted from the competition between PCA's stability and the severity of hydrothermal condition. Besides, the interactions between quaternary ammonium groups and aluminosilicate species may also have a stabilization effect to preserve the PCA structure. As has been reported in previous studies, cationic PDADMAC is more stable in zeolite precursor (pH = 14, large-sized fused silica) than in NaOH solution at the same hydrothermal temperature (180 °C) [48], which is a direct evidence for the stabilization effect of zeolite precursor on cationic polymer. Compared with vulnerable PCA in this work, PDADMAC has high stability because PDADMAC not only has other stable C-C bonds to link the backbone chain even after cleavage of the C-N bonds of quaternary ammonium groups, but also possesses high charge density and high accessibility of cationic charges to readily attract large-sized aluminosilicate species to stabilize its quaternary ammonium groups.

Comparing with PCA-Silicalite-1 and PCA-ZSM-5 (Seed), it can be described that the significant templating effect of the vulnerable PCA in PCA-ZSM-5 is benefited from the well-chosen synthetic condition to a greater extent, namely the negatively charged and small-sized nanoblocks in zeolite precursor. Generally speaking, PCA may not possess as adequate stability and high charge density as the previously reported cationic polymers,[25-28] but can successfully serve as a meso-template in certain cases and well illustrate some important issues in the synthesis of hierarchical zeolites.

Aluminum coordination, acidity and catalytic performance of PCA-ZSM-5 and other counterparts

95 We continue to track the aluminum coordination, acidity and catalytic performance of the abovementioned three representative materials, *i.e.*, NCA-ZSM-5, PCS-ZSM-5 and PCA-ZSM-5.

As illustrated in Fig. S13, ^{27}Al MAS NMR spectroscopy of

15 conditions suggest that the zeolite precursor should be associated with the polymer-silica interactions and thus influences the templating effect of PCA during zeolite crystallization. In the synthesis of PCA-ZSM-5, TEOS and small amount of aluminum isopropoxide hydrolyze and condense to produce small-sized nanoblocks.[45] Then PCA can well assemble with and be encapsulated within the aluminosilicate species composed of nanoblocks. There is no competition between the assembly of small-sized precursor with polymer PCA and TPAOH-directed zeolite crystallization, which is beneficial for generating mesopores within crystalline ZSM-5 zeolite during hydrothermal treatment. However, in the case of PCA-ZSM-5 (Seed), although PCA as a mesoscale polymer has no size mismatch with the large particles of zeolite seeds (average particle size is 10 nm, Fig. S12) [46], its limited charge density, caused by the wide separation of cationic centers, is responsible for the failure in enough interactions with the negatively charged and large-sized zeolite seeds. Therefore, PCA does not well assemble with zeolite seeds and may undergo decomposition of more quaternary ammonium groups due to more exposure to the harsh hydrothermal condition. The shortcoming of cationic PCA somewhat resembles that of TMB-swollen mesoscale surfactant micelles (TMB: 1,3,5-trimethylbenzene), which also has insufficient interactions with bulky aluminosilicate species due to limited charge density.[47] Besides, 3D geometry of long chain in PCA may causes low proportion of accessible quaternary ammonium groups / cationic charges for large-sized zeolite seeds, which is also responsible for the insufficient interaction between PCA and zeolite seeds. High charge density and/or high accessibility of cationic charges has been achieved by cationic ammonium-modified chitosan (HTCC) assembling with zeolite seeds about several nanometers[28] and polydiallyldimethylammonium chloride (PDADMAC) assembling with large nanocrystals about 30-80 nm.[46] Therefore, the effective interactions between quaternary ammonium groups and negatively charged aluminosilicate species facilitate the templating effect of PCA. Although PCA is partially decomposed during zeolite crystallization, it has residual cationic charges and macromolecular structure, which are still able to allow significant templating effect on PCA-ZSM-5. PCS also has abundant charges to exert sufficient Coulomb interaction, but unfortunately the cationic centers are too close, resulting in fast destructive decomposition and small decomposed products which can not sustain mesopores during zeolite crystallization.

calcined NCA-ZSM-5, PCS-ZSM-5 and PCA-ZSM-5 exhibit an intense signal at around 54 ppm, owing to tetrahedrally coordinated framework aluminum. Besides, all three materials show a weak signal centered at around 0 ppm, which can be attributed to octahedral extraframework aluminum species and thus demonstrates that most Al atoms in the three materials are incorporated into the framework. The addition of PCS or PCA does not significantly influence the aluminum coordination.

Similar acidic features of the three samples are observed by their look-alike NH_3 -TPD curve profile, as shown in Fig. S14. Considering the intensity of signals, PCA-ZSM-5 has similar number and strength of acid sites to the NCA-ZSM-5. However, PCS-ZSM-5 has significantly higher number of strong acidic sites (at 300-600 °C) than NCA-ZSM-5 and PCA-ZSM-5, because the latter two have higher Si/Al ratio and possess more mesopores, which reduce the number of acidic sites [49].

Catalytic performance results of the three materials are given in Table 2 and Figure S15. Catalytic activity for the acetalization of cyclohexanone with methanol (ACM, Fig. 8) is relatively high within 1 hour, and increases slowly until the reaction achieves balance (Fig. S15a) due to the blockage of active sites by product molecules [50]. Table 2 provides the conversions of cyclohexanone over various catalysts at 1 h. They follow the order of PCS-ZSM-5 (85.4%) > PCA-ZSM-5 (84.3%) > PCS-ZSM-5 (80.6%). The bulky PCS-ZSM-5 with the lowest mesoporosity and highest acid content has higher activity than NCA-ZSM-5 and PCA-ZSM-5, which reveals that the catalytic activity for the small molecular ACM reaction is closely related to the concentration/strength of acid sites characterized by the NH_3 -TPD. [51] Based on comparable acidity, PCA-ZSM-5 is slightly more active than NCA-ZSM-5, which is benefited from the shortened diffusion path within the hierarchical PCA-ZSM-5 particles. Generally, the small molecular reactants do not have very severe diffusion constraints, and hence the enhanced mesoporosity will not induce significant improvement in catalytic activity [51].

When the aldol condensation of benzaldehyde with n-butyl alcohol (CBB, Fig. 8), a large molecular reaction, was tested on these samples, the results are different from ACM reaction. The conversions for CBB at 4 h over various catalysts are listed in Table 2. The catalytic activities for CBB follow the order of PCA-ZSM-5 (39.2%) > NCA-ZSM-5 (33.3%) > PCS-ZSM-5 (23.7%), which is in line with the order of mesoporosity (Table 1). Higher mesoporosity allows more efficient intraparticle diffusion of bulky molecules and creates more accessible acid sites for bulky molecules. The large size of mesopores (7-50 nm) may be also conducive to the catalytic activity of PCA-ZSM-5 [52]. PCS-ZSM-5 with the lowest mesoporosity imposes the most severe diffusional and steric limitations on large reactants, leading to its lowest catalytic activity. By contrast, the highest acid content of PCS-ZSM-5 does not conspicuously contribute to its catalytic activity for the large molecular CBB reaction. The not-so-large difference of catalytic activity among PCA-ZSM-5, PCS-ZSM-5 and NCA-ZSM-5 can be explained that a certain degree of mesoporosity in PCS-ZSM-5 ($0.17 \text{ cm}^3/\text{g}$) and NCA-ZSM-5 ($0.27 \text{ cm}^3/\text{g}$) facilitates their respective activity to different extent. The effect of reaction time on catalytic activity is shown in Fig.

S15b, which indicates a larger conversion difference at longer reaction time.

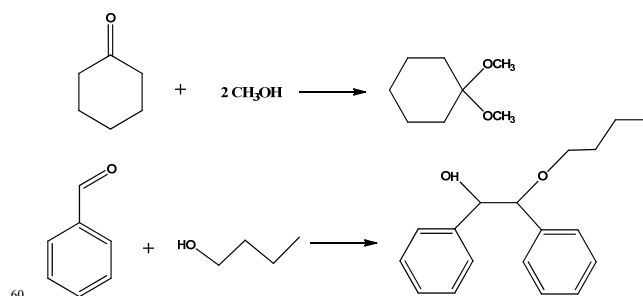


Fig. 8 Acetalization of cyclohexanone with methanol (top); aldol condensation of benzaldehyde with n-butyl alcohol (bottom).

Table 2 Catalytic performance of various ZSM-5 catalysts.

Sample	Si/Al ^a	Catalytic activity ^b	
		ACM (1 h)	CBB (4 h)
NCA-ZSM-5	49.3	80.6%	33.3%
PCS-ZSM-5	42.1	85.4%	23.7%
PCA-ZSM-5	51.4	84.3%	39.2%

^a The numbers indicate Si/Al ratio obtained by ICP-OES analysis; ^b Catalytic activity for ACM is indicated by cyclohexanone conversion, while catalytic activity for CBB is indicated by benzaldehyde conversion; the selectivity to target product molecule is close to 100 %.

Conclusions

When assembling with small-sized nanoblocks to synthesize hierarchical ZSM-5, the easily available cationic polymer PCA undergoes partial hydrothermal decomposition and successfully creates mesopores ranging between 7 and 50 nm in the ZSM-5 particle. However, PCS does not serve as a meso-template due to complete decomposition and results in bulky zeolite particles with low mesoporosity, which is inferior to NCA-ZSM-5 synthesized without polymer and exhibiting nanocrystallite aggregates. The significant templating effect of PCA compared with PCS is because the cationic centers of are widely separated by more than three carbons, which contributes to the improved stability of PCA during zeolite crystallization. However, PCA can not assemble with large-sized zeolite seeds and template mesopores in ZSM-5, because the limited charge density of PCA only provides insufficient interactions with zeolite seeds. Catalytic activity for the aldol condensation of benzaldehyde with n-butyl alcohol involving large molecules follows the order of PCA-ZSM-5 > NCA-ZSM-5 > PCS-ZSM-5, consistent with the order of mesoporosity. However, although PCA-ZSM-5 and NCA-ZSM-5 have rich mesoporosity, they are less active than PCS-ZSM-5 for the acetalization of cyclohexanone with methanol involving small-sized reactants, due to the lower number of acidic sites. Inspired by the application of PCA, it is believed that other easily available cationic polymers with quaternary ammonium groups in the long polymer chain may also be applicable to the templating synthesis of hierarchical ZSM-5.

Acknowledgements

X. G. Zhou is grateful for financial support from the National Basic Research Program of China (2012CB720501) and the Natural Science Foundation of China (U1162112). K. K. Zhu is

sponsored by New Century Excellent Talents in University (NCET-11-0644) of the Chinese Department of Education.

Notes and references

- ^a State Key Laboratory of Chemical Engineering, East China University of Science and Technology, Shanghai, 200237, P. R. China. Fax: +86 21 64253528; Tel: +86 21 64253509; E-mail: xgzhou@ecust.edu.cn
- † Electronic Supplementary Information (ESI) available: [details of any supplementary information available should be included here]. See DOI: 10.1039/b000000x/
- ‡ Footnotes should appear here. These might include comments relevant to but not central to the matter under discussion, limited experimental and spectral data, and crystallographic data.
1. A. Corma, *Chem. Rev.*, 1997, **97**, 2373.
 2. J. Perez-Ramirez, C. H. Christensen, K. Egeblad, C. H. Christensen and J. C. Groen, *Chem. Soc. Rev.*, 2008, **37**, 2530.
 3. S. Mintova, J.-P. Gilson and V. Valtchev, *Nanoscale*, 2013, **5**, 6693.
 4. A. Corma, V. Fornes, S. B. Pergher, T. L. M. Maesen and J. G. Buglass, *Nature*, **1998**, 396, 353.
 5. M. Choi, K. Na, J. Kim, Y. Sakamoto, O. Terasaki and R. Ryoo, *Nature*, 2009, **461**, 246.
 6. S. Lopez-Orozco, A. Inayat, A. Schwab, T. Selvam and W. Schwieger, *Adv. Mater.*, 2011, **23**, 2602.
 7. J. Lynch, F. Raatz and P. Dufresne, *Zeolites*, 1987, **7**, 333.
 8. M. M. L. Ribeiro Carrott, P. A. Russo, C. Carvalhal, P. J. M. Carrott, J. P. Marques, J. M. Lopes, I. Gener, M. Guisnet and F. Ramôa Ribeiro, *Microporous Mesoporous Mater.*, 2005, **81**, 259.
 9. S. Abelló, A. Bonilla and J. Pérez-Ramírez, *Appl. Catal., A*, 2009, **364**, 191.
 10. X. Meng, F. Nawaz and F.-S. Xiao, *Nano Today*, 2009, **4**, 292.
 11. K. Egeblad, C. H. Christensen, M. Kustova and C. H. Christensen, *Chem. Mater.*, 2007, **20**, 946.
 12. C. J. H. Jacobsen, C. Madsen, J. Houzvicka, I. Schmidt and A. Carlsson, *J. Am. Chem. Soc.*, 2000, **122**, 7116.
 13. W. Fan, M. A. Snyder, S. Kumar, P.-S. Lee, W. C. Yoo, A. V. McCormick, R. Lee Penn, A. Stein and M. Tsapatsis, *Nat. Mater.*, 2008, **7**, 984.
 14. I. Schmidt, A. Boisen, E. Gustavsson, K. Ståhl, S. Pehrson, S. Dahl, A. Carlsson and C. J. H. Jacobsen, *Chem. Mater.*, 2001, **13**, 4416.
 15. H. Zhu, Z. Liu, Y. Wang, D. Kong, X. Yuan and Z. Xie, *Chem. Mater.*, 2007, **20**, 1134.
 16. J. Zhou, Z. Hua, Z. Liu, W. Wu, Y. Zhu and J. Shi, *ACS Catal.*, 2011, **1**, 287.
 17. F. Schmidt, S. Paasch, E. Brunner and S. Kaskel, *Microporous Mesoporous Mater.*, 2012, **164**, 214.
 18. Y. Zhu, Z. Hua, J. Zhou, L. Wang, J. Zhao, Y. Gong, W. Wu, M. Ruan and J. Shi, *Chem.–Eur. J.*, 2011, **17**, 14618.
 19. M. Choi, H. S. Cho, R. Srivastava, C. Venkatesan, D.-H. Choi and R. Ryoo, *Nat. Mater.*, 2006, **5**, 718.
 20. J. Yao, Y. Huang and H. Wang, *J. Mater. Chem.*, 2010, **20**, 9827.
 21. H. Zhu, Z. Liu, D. Kong, Y. Wang and Z. Xie, *J. Phys. Chem. C*, 2008, **112**, 17257.
 22. Y. Tao, H. Kanoh and K. Kaneko, *Langmuir*, 2004, **21**, 504.
 23. H. Wang and T. J. Pinnavaia, *Angew. Chem. Int. Ed.*, 2006, **45**, 7603.
 24. D. H. Park, S. S. Kim, H. Wang, T. J. Pinnavaia, M. C. Papapetrou, A. A. Lappas and K. S. Triantafyllidis, *Angew. Chem.*, 2009, **121**, 7781.
 25. F.-S. Xiao, L. Wang, C. Yin, K. Lin, Y. Di, J. Li, R. Xu, D. S. Su, R. Schlögl, T. Yokoi and T. Tatsumi, *Angew. Chem.*, 2006, **118**, 3162.
 26. L. Wang, Z. Zhang, C. Yin, Z. Shan and F.-S. Xiao, *Microporous Mesoporous Mater.*, 2010, **131**, 58.
 27. F. Liu, T. Willhammar, L. Wang, L. Zhu, Q. Sun, X. Meng, W. Carrillo-Cabrera, X. Zou and F.-S. Xiao, *J. Am. Chem. Soc.*, 2012, **134**, 4557.
 28. J. Jin, X. Zhang, Y. Li, H. Li, W. Wu, Y. Cui, Q. Chen, L. Li, J. Gu, W. Zhao and J. Shi, *Chem.–Eur. J.*, 2012, **18**, 16549.
 29. L. Han, J. Yao, D. Li, J. Ho, X. Zhang, C.-H. Kong, Z.-M. Zong, X.-Y. Wei and H. Wang, *J. Mater. Chem.*, 2008, **18**, 3337.

30. J. Yao, H. Wang, S. P. Ringer, K.-Y. Chan, L. Zhang and N. Xu, *Microporous Mesoporous Mater.*, 2005, **85**, 267.
31. M. Fujiwara, A. Sakamoto, K. Shiokawa, A. K. Patra and A. Bhaumik, *Microporous Mesoporous Mater.*, 2011, **142**, 381.
32. W. Jaeger, J. Bohrich and A. Laschewsky, *Prog. Polym. Sci.*, 2010, **35**, 511.
33. B. Bauer, H. Strathmann and F. Effenberger, *Desalination*, 1990, **79**, 125.
34. W. Chaikittisilp, Y. Suzuki, R. R. Mukti, T. Suzuki, K. Sugita, K. Itabashi, A. Shimojima and T. Okubo, Organized, *Angew. Chem. Int. Ed.*, 2013, **52**, 3355.
35. L. Ghimici, I. Dranca, S. Dragan, T. Lupascu and A. Maftuleac, *Eur. Polym. J.*, 2001, **37**, 227.
36. S. H. Lee, M. C. Shin, S. J. Choi, J. H. Shin and L. S. Park, *Environ. Technol.*, 1998, **19**, 431.
37. J.-H. Choi, W. S. Shin, S.-H. Lee, D.-J. Joo, J.-D. Lee, S. J. Choi and L. S. Park, *Sep. Sci. Technol.*, 2001, **36**, 2945.
38. Eur. Pat., 0549925A1, 1993
39. H. van Koningsveld, J. C. Jansen and H. van Bekkum, *Zeolites*, 1990, **10**, 235.
40. R. R. Mukti, H. Hirahara, A. Sugawara, A. Shimojima and T. Okubo, *Langmuir*, 2009, **26**, 2731
41. W. Park, D. Yu, K. Na, K. E. Jelfs, B. Slater, Y. Sakamoto and R. Ryoo, *Chem. Mater.*, 2011, **23**, 5131.
42. S. Drään and L. Ghimici, *Angew. Makromol. Chem.*, 1991, **192**, 199.
43. M. S. Gibson, in *The Amino Group*, ed. Saul Patai, John Wiley & Sons, New York, 1968, ch.2, pp. 46-50.
44. S. Dragan and M. Cristea, *Eur. Polym. J.*, 2001, **37**, 1571.
45. R. Ravishankar, C. E. A. Kirschhock, P.-P. Knops-Gerrits, E. J. P. Feijen, P. J. Grobet, P. Vanoppen, F. C. De Schryver, G. Miehe, H. Fuess, B. J. Schoeman, P. A. Jacobs and J. A. Martens, *J. Phys. Chem. B*, 1999, **103**, 4960.
46. J. Song, L. Ren, C. Yin, Y. Ji, Z. Wu, J. Li and F.-S. Xiao, *J. Phys. Chem. C*, 2008, **112**, 8609.
47. F. N. Gu, F. Wei, J. Y. Yang, N. Lin, W. G. Lin, Y. Wang and J. H. Zhu, *Chem. Mater.*, 2010, **22**, 2442.
48. J. Zhu, Y. Zhu, L. Zhu, M. Rigutto, A. van der Made, C. Yang, S. Pan, L. Wang, L. Zhu, Y. Jin, Q. Sun, Q. Wu, X. Meng, D. Zhang, Y. Han, J. Li, Y. Chu, A. Zheng, S. Qiu, X. Zheng and F.-S. Xiao, *J. Am. Chem. Soc.*, 2014, **136**, 2503.
49. X. Zhou, H. Chen, Y. Zhu, Y. Song, Y. Chen, Y. Wang, Y. Gong, G. Zhang, Z. Shu, X. Cui, J. Zhao, and J. Shi, *Chem.–Eur. J.*, 2013, **19**, 10017.
50. B. Thomas, S. Prathapan and S. Sugunan, *Appl. Catal., A*, 2004, **277**, 247.
51. R. Srivastava, N. Iwasa, S.-i. Fujita and M. Arai, *Chem.–Eur. J.*, 2008, **14**, 9507.
52. H. Li, J. Jin, W. Wu, C. Chen, L. Li, Y. Li, W. Zhao, J. Gu, G. Chen, and J. Shi, *J. Mater. Chem.*, 2011, **21**, 19395.